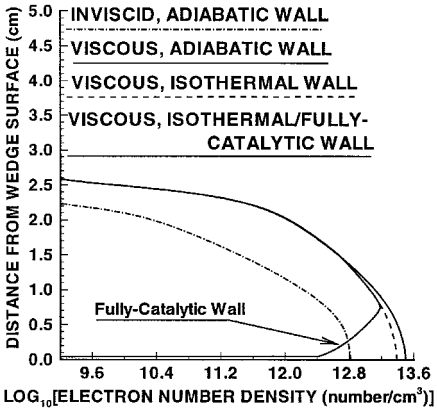

Fig. 3 Electron number density profiles for nonequilibrium inviscid and viscous flow over a blunt wedge (20 cm from the leading edge).

weakened, producing a smaller density gradient across the shock. Viscosity also increases chemical dissociation near the wall; n_{el} is most affected since recombination with NO^+ is inhibited by the release of thermal energy in the flow near the wall. Signal attenuation predicted for inviscid flow is 10.7 dB, and for viscous flow it is 16.6 dB. The viscous flow value more closely matches the measured value of 18 dB. Peak electron number densities shown in Fig. 3 ($n_{el,pk} > 5 \times 10^{12}$ cm^{-3}) are larger than the critical density $n_{el,crit}$ of 9×10^8 cm^{-3} for $\omega = 1.7$ GHz. As noted earlier, this is the situation (i.e., $n_{el,pk} >> n_{el,crit}$) for which the present EM model is accurate. Additional results for an isothermal body surface (freestream temperature) are also shown in Fig. 3. Noticeably smaller values for n_{el} are computed near the isothermal wall; divergence of the curves begins between the body surface and the bow shock. A signal attenuation of 16 dB predicted for the isothermal wall is smaller than that for the adiabatic wall, cited earlier. The wedge model used in the Boyer study was metallic and it is well known that metallic surfaces catalyze chemical reactions in air, therefore, computations were performed for viscous flow and an isothermal, fully catalytic wall (see Fig. 3). Because of enforced equilibrium, e^- recombination with NO^+ is promoted near the wall ($n_{el} \approx 0$, $\log_{10}(n_{el}) \approx -10$). Note the similarity of the profile shape in Fig. 3 for a fully catalytic wall and that shown in Fig. 1. A signal attenuation level of 15.8 dB predicted for the fully catalytic isothermal wall is smaller than that for a noncatalytic adiabatic wall.

Conclusions

Flow viscosity is an important factor in achieving close comparison between measured and computed signal attenuation since the electron distribution in the shock/boundary layer is much larger than that for inviscid flow. An adiabatic wall yields a greater number of flow electrons as compared to an isothermal wall, producing the largest degree of attenuation. A catalytic wall reduces electron number density and reduces attenuation.

Acknowledgments

This work was supported by the U.S. Army Research Laboratory, the Department of Defense High Performance Computing Research Initiative, and was overseen by J. D. Anderson Jr. of the University of Maryland.

References

[1]Heald, M., and Wharton, C., *Plasma Diagnostics with Microwaves*, Wiley, New York, 1965, pp. 4–12.

[2]Glick, H., "Interaction of Electromagnetic Waves with Plasmas of Hypersonic Flows," *ARS Journal*, Vol. 32, No. 9, 1962, pp. 1359–1364.

[3]Gal, G., "Electromagnetic Wave Propagation in a Lossy Plasma Slab with a Gradient Transverse to the Incident Wave," NASA SP-252, May 1971.

[4]Nusca, M., "Investigation of Ram Accelerator Flows for High Pressure Mixtures of Various Chemical Compositions," AIAA Paper 96-2946, July 1996.

[5]Dunn, M., and Kang, S.-K., "Theoretical and Experimental Studies of Reentry Plasmas," NASA CR-2232, April 1973.

[6]Chapman, S., and Cowling, T., *The Mathematical Theory of Non-Uniform Gases*, Cambridge Univ. Press, Cambridge, England, UK, 1970, pp. 111, 271.

[7]Chadwick, K., Boyer, D., and Andre, S., "Plasma and Flowfield Induced Effects on Hypervelocity Re-Entry Vehicles for L-Band Irradiation at Near Broadside Aspect Angles," AIAA Paper 96-2322, June 1996.

[8]Hill, P., and Peterson, C., *Mechanics and Thermodynamics of Propulsion*, Addison–Wesley, Reading, MA, 1965, pp. 111, 112.

[9]Shen, J., and Qu, Z., "Numerical Study of Non-Equilibrium Flowfield Coupled with Electric Field," AIAA Paper 95-6070, April 1995.

[10]Marion, J., and Heald, M., *Classical Electromagnetic Radiation*, 2nd ed., Harcourt Brace Jovanovich, New York, 1980, pp. 144–146.

[11]Epstein, M., "Interaction of High Power Microwaves with a Reentry Vehicle Plasma Sheath," *Transactions of the 8th Symposium on Ballistic Missile and Space Technology*, Vol. II, Academic, New York, 1963, pp. 97–119.

[12]Ohler, S., Ruffin, A., Gilchrist, B., and Gallimore, A., "RF Signal Impact Study of an SPT," AIAA Paper 96-2706, July 1996.

[13]Boyer, D., Bein, G., and Andre, S., "Studies of Microwave Transmission Through a Hypersonic Air Plasma," Sandia Rept., SC-CR-67-2710, June 1967.

Quasi-Steady-State Performance of a Heat Pipe Subjected to Transient Acceleration Loadings

Scott K. Thomas*
Wright State University, Dayton, Ohio 45435
and
Kirk L. Yerkes†
U.S. Air Force Wright Laboratory,
Wright–Patterson Air Force Base, Ohio 45433-7251

Introduction

THE analysis of heat pipes has usually been restricted to the inclusion of a static acceleration field, such as that caused by gravity. While this analysis is appropriate in many applications, it is not valid in the assessment of the thermal performance of heat pipes in acceleration fields that are varying with time. For instance, heat pipes have been proposed to be used aboard fighter aircraft such as the U.S. Navy F/A-18 to act as heat sinks for electronics packages that drive aileron or trailing-edge flap actuators.[1–3] During combat, transient acceleration fields of up to 9 *g* will be present on the aircraft. Therefore, knowledge of the thermal performance of heat pipes under transient acceleration loadings is of importance to designers of the electronics packages in need of cooling. The objective of the present experimental investigation is to determine the quasi-steady-state thermal resistance of a flexible copper-water heat pipe under transient acceleration loadings

Received June 27, 1996; revision received Oct. 4, 1996; accepted for publication Oct. 9, 1996.

*Assistant Professor, Department of Mechanical and Materials Engineering. Member AIAA.

†Research Engineer, Thermal Technology Section, WL/POOS-3. Member AIAA.

with constant heat input. The performance of the heat pipe is examined for the following parameter ranges: heat input Q_e = 75–150 W; condenser temperature T_c = 3, 20, and 35°C; and acceleration frequency f = 0, 0.01, 0.05, 0.1, 0.15, and 0.2 Hz. The centrifuge radial acceleration loadings ranged from 1.1 to 9.8 g for each frequency setting. In addition, the effects of the previous dryout history are noted.

Experimental Setup

Determination of the thermal resistance of the flexible copper-water heat pipe under transient radial acceleration loadings was accomplished by placing the pipe onto a 2.44-m-diam centrifuge table.[2] The heat pipe was mounted along a circular path at a radius of 1.149 m from the central axis of the centrifuge table. Transient acceleration fields were imposed on the heat pipe via open-loop control of the centrifuge angular velocity by a waveform generator, which fed signals to the motor. The angular velocity of the centrifuge table was sinusoidal, ω = sin ft, but the radial acceleration was a sine-squared function given by $a_r = r\omega^2 = r \sin^2 ft$. While the acceleration fields on an aircraft are made up of many harmonics, information can be gathered over a range of frequencies for a single harmonic waveform to study the frequency response of the system. In this way, a performance envelope can be developed that can be used by designers of the electronic packages. The 20-hp dc electric motor was capable of maintaining a proper waveform on the table up to frequencies of f = 0.2 Hz, which dictated the upper end of the frequency testing. At higher frequencies, the response of the table was such that the imposed acceleration was attenuated from the desired range of 1.1 to 9.8 g. The acceleration field at the heat pipe location was measured by a triaxial accelerometer with an uncertainty of ±0.1 g. Input power was supplied to the heat pipe from a precision power supply through power slip rings to the table. The input power was read by a power analyzer that had an uncertainty of ±1 W. A thermofoil heater was attached to the evaporator mounting plate. Cooling fluid was delivered to the condenser mounting plate via a hydraulic rotary coupling. The temperature of the cooling fluid was maintained at a constant setting by a recirculating chiller to within ±0.5°C. The mass flow rate of the coolant was measured by a calibrated rotameter to an uncertainty of ±0.02 kg/min. Heat pipe temperatures were measured by type T thermocouples (±0.5°C). Temperature signals were amplified and conditioned on the centrifuge table. These signals were transferred off the table through instrumentation slip rings, which were completely separate from the power slip rings to reduce noise. Conditioning the temperature signals prior to leaving the centrifuge table eliminated difficulties associated with creating additional junctions within the slip-ring assembly. Temperature and acceleration signals were collected using a personal computer and data logging software. Information concerning the heat pipe is given by Yerkes and Beam.[2]

Test Procedure

The flexible copper-water heat pipe was tested in the following manner. The recirculating chiller was turned on and allowed to reach the set point temperature. The centrifuge table was started from the remote control room at a slow constant rotational speed (f = 0) to prevent damage to the power and instrumentation slip rings. Power to the heater was applied, and the heat pipe was allowed to reach a steady-state condition, which was determined by monitoring various temperatures on the heat pipe. The centrifuge table angular velocity was then changed to a sinusoidal waveform. The frequency of the waveform driving the centrifuge table was increased in steps (f = 0.01, 0.05, 0.1, 0.15, and 0.2 Hz), with steady conditions being reached at each setting. After all data had been recorded, the power to the heater was turned off and the heat pipe allowed to cool before shutting down the centrifuge table. The thermal resistance of the heat pipe, defined as the evaporator-to-condenser temperature difference divided by the heat input, was calculated for each steady-state condition, $R_{th} = (T_e - T_c)/Q_e$, where T_e and T_c are the temperatures nearest the evaporator and condenser end caps,[2] respectively. Calorimetric tests were performed and it was determined that the difference between the heat input to the evaporator and that extracted by the condenser was less than 10%, and so the heat input is used for data reduction. The maximum uncertainty of the reported thermal resistance data was calculated to be $\pm 9.5 \times 10^{-3}$ K/W. The repeatability of the data was examined and the maximum difference in the thermal resistance observed between two identical runs was 7%.

Results and Discussion

The performance characteristics of a flexible copper-water heat pipe under transient radial acceleration loadings have been determined using a centrifuge table. The thermal resistance of the heat pipe was measured while varying the following parameters: the acceleration frequency, evaporator heat input, and condenser temperature. The raw data from a typical set of tests are shown in Fig. 1. The overall temperature difference across the heat pipe was slightly higher under the imposed transient acceleration field, as opposed to that for no acceleration (f = 0). Also, the temperature difference decreased as the centrifuge table frequency increased. This was a result of the fluid within the heat pipe sloshing from the condenser to the evaporator section, which effectively cooled the evaporator by supplying additional fluid above that delivered by the capillary wick structure. For the lower heat inputs (Figs. 1a and

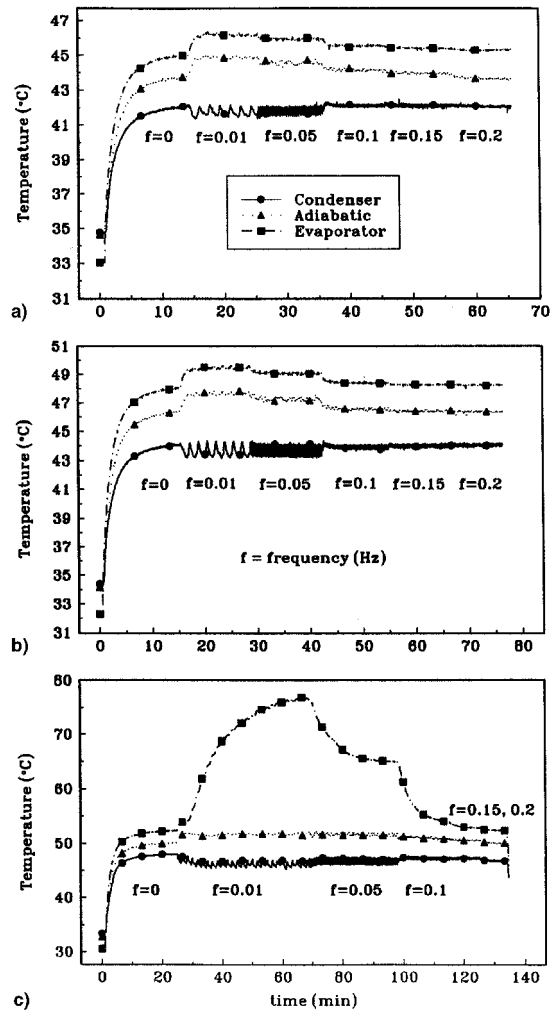

Fig. 1 Temperature vs time for T_c = 35°C and various frequency settings. Q_e = a) 75, b) 100, and c) 137 W.

Table 1 Overtemperature dryout conditions for the flexible copper-water heat pipe

T_c, °C	f, Hz	Q_e, W
3	0	≥150
3	0.01	≥113
3	0.05	≥125
3	0.1	≥137
3	0.15	≥137
3	0.2	≥137
20	0.01	≥137
20	0.05	≥150

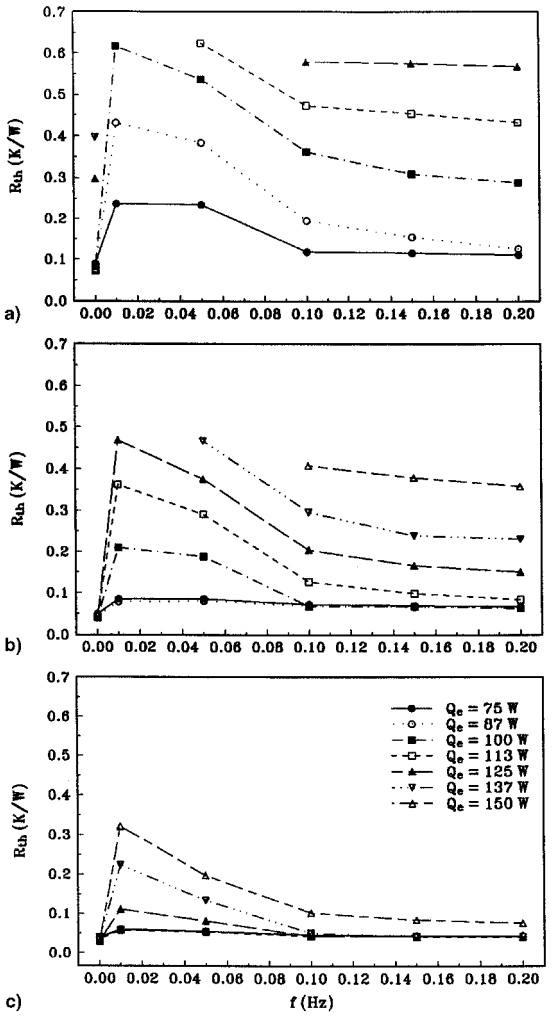

Fig. 2 Thermal resistance vs frequency for various heat inputs. T_c = a) 3, b) 20, and c) 35°C.

1b), the overall temperature difference did not change appreciably. For the higher heat input (Fig. 1c), the thermal resistance was significantly higher for the case of $f = 0.01$ Hz. At this point, the outboard evaporator pad temperature (closest to the evaporator end cap) exceeded the inboard temperature (closest to the adiabatic section), which was defined as a partial evaporator dryout condition. In some cases, the evaporator temperature exceeded $T_e = 100$°C, which was defined as an overtemperature dryout condition. Because of limitations of the instrumentation and the impracticality of allowing electronic components to reach such a high temperature, a steady-state overtemperature condition was not attempted. Table 1 presents the conditions under which the heat pipe experienced an overtemperature dryout condition. With no acceleration ($f = 0$), the heat pipe dried out at $Q_e = 150$ W for the lowest condenser temperature ($T_c = 3$°C). The heat input at which dryout occurred when the transient acceleration field was imposed decreased significantly for the lowest frequency settings. In these cases, the time period during which the heat pipe was tangentially accelerating and decelerating was relatively long. This resulted in a liquid pool that alternately resided in the condenser section and evaporator section for a significant amount of time. When the pool was in the condenser, the evaporator reached a partial dryout condition that was not recovered from when the liquid pool returned to the evaporator, because the significant overheating impaired the ability of the fluid to rewet the evaporator wick. The power input at which overtemperature dryout occurred increased with the centrifuge table frequency for both condenser temperatures. Overtemperature dryout was not encountered for $T_c = 35$°C. The test results for the stationary heat pipe ($f = 0$) are presented graphically in Fig. 2. The thermal resistance was nearly constant for condenser temperatures of $T_c = 20$ and 35°C, but increased significantly with heat input after $Q_e = 113$ W for $T_c = 3$°C. This reduction in the capillary limit with operating temperature resulting from property variations is well documented in the heat pipe literature.[4–6] The heat pipe thermal resistance for the case of increasing frequency is also shown in Fig. 2. In general, the thermal resistance decreased as the table frequency increased, particularly above values of $f = 0.1$ Hz. This may be indicative of a type of resonance within the heat pipe system where the effects of fluid slosh and partial dryout were affecting the performance of the pipe. This particular phenomenon will be addressed in future analytical studies. The heat pipe thermal resistance also decreased as the condenser temperature increased. Therefore, the condenser section should reject heat to conditions that can maintain the operating temperature of the heat pipe significantly above the freezing temperature of the working fluid.

Partial Dryout Results

During the course of experimentation, it was discovered that the thermal resistance of the flexible copper-water heat pipe was dependent on the previous dryout conditions. This phenomenon is elucidated by examining the following set of tests, where the input power was $Q_e = 137$ W and the coolant temperature was $T_c = 20$°C. Figure 3a shows a typical test for the thermal characteristics of the flexible heat pipe (test 1), where the centrifuge table frequency was increased throughout the test ($f = 0$, 0.05, 0.1, 0.15, and 0.2 Hz). In Fig. 3b, the table frequency was varied as follows: $f = 0$, 0.15, 0.1, 0.05, and 0.1 Hz (test 2). Figure 3c presents the results for test 3, where the frequency variation was $f = 0$, 0.2, 0.15, 0.1, 0.05, and 0.1 Hz. After the steady state was reached in test 3 at $f = 0.1$ Hz, the input power was shut off, and the heat pipe was allowed to cool and the evaporator wick to reprime fully before restarting the pipe. Table 2 summarizes the results of the three tests. The repeatability of the results are excellent, as can be seen in the evaporator temperatures for $f = 0.05$ Hz ($T_e = 97.0$, 99.4, and 97.0°C). In addition, the transition from $f = 0.05$ to 0.1 Hz is also repeatable ($T_e = 75.1$, 74.2, and 75.1°C for $f = 0.1$ Hz). Upon examination of the results for $f = 0.1$ Hz, it can be seen that the evaporator temperature is dependent on the previous temperature history of the heat pipe. For example, in tests 1 and 3, the transition from $f = 0.05$ to 0.1 results in evaporator temperatures of $T_e = 75.1$°C at $f = 0.1$ Hz for each test. However, the transition from $f = 0.15$ to 0.1 Hz, shown in tests 2 and 3, gives $T_e = 54.7$ and 54.0°C, respectively (at $f = 0.1$ Hz). Similar results can be found for $f = 0.15$ Hz ($T_e = 67.8$°C for $f = 0.1$–0.15 Hz and $T_e = 42.3$°C for $f = 0.2$–0.15 Hz). In both cases, when the heat pipe did not experience a partial dryout at the previous frequency setting, the evaporator temperature was lower than when a partial dryout was present at the previous setting. In other words, if the evaporator temperature shows a partial dryout condition, increasing the frequency will decrease the evaporator temperature, but not as much as if no dryout was present. Therefore, the thermal re-